ACOUSTIC AND MAGNETIC PROPERTIES OF MAGNETIC LIQUIDS

A. SKUMIEL, T. HORNOWSKI and A. JÓZEFCZAK

Institute of Acoustics
Adam Mickiewicz University
(60-769 Poznań, Matejki 48/49)
e-mail: skumiel@main.amu.edu.pl

The influence of magnetic field on the acoustic and magnetic properties of magnetic liquids is discussed. By fitting the curve of Taketomi's theory to the experimental data of the anisotropy of ultrasonic attenuation, the values of quantities describing the structure of magnetic liquid have been determined. Moreover, the dependence of magnetic susceptibility on frequency has been measured. It shows that two processes of magnetization, which are based on the mechanisms proposed by Brown and Néel, contribute to the magnetization of the EMG-605 magnetic liquid.

1. Introduction

Magnetic liquids do not exist in nature. They owe their existence to recent developments in the technology of materials and the concomitant applications in the computer technique, medicine, modern military setups, as well as in the instruments of every-day usage.

In this paper an attempt is made to elucidate the influence of an external magnetic field on the propagation of ultrasonic waves and the magnetic properties of magnetic liquids. The field gives rise to anisotropy: the liquid undergoes restructurization by the formation of spherical and chain-like clusters. As a result, the absorption of the wave undergoes an enhancement due to the rotational and translational motions of the clusters.

Moreover, it was our aim to determine which of those mechanisms predominates under different external conditions and to gain as much information as possible concerning the structure of magnetic liquids, in particular concerning the radius of the spherical clusters and their concentration. A magnetic liquid is defined as a colloid suspension of magnetic particles in a carrier liquid (water, mineral oil, or an organic compound). The radii of magnetic particles (grains) typically range from 5 to 10 nm. They are involved in Brownian motion, and their smallness considerably restricts the natural process of gravitational sedimentation.

Coagulation of the individual magnetic particles leads to a restructurizarion of the magnetic liquid. Spherical clusters arise with radii ranging from some tens of nanometers

up to several micrometers as well as chain-like clusters that can be observed by a micro-scope. In the external magnetic field the chain-like clusters array themselves along the lines of the field increasing the stiffness of the liquid and modyfying its acoustic proper-ties. The size of the spherical clusters as well as the length of the chains they form are primarily dependent on the magnetic field strength and the temperature. The magnetic liquid EMG-605, which was studied by authors, consisted of water (as the carried liquid) and suspended particles of $FeO \cdot Fe_2O_3$ with diameters of about 20 nm. Thus, we dealt with a colloidal solution having a high degree of dispersion and containing polydisperse ferrimagnetic particles endowed with an intrinsic magnetic moment.

In the majority of magnetic liquids the state of magnetization is rather well described by the Langevin's law for the magnetization of molecules of a paramagnetic gas. However, in magnetic liquids the effective state of magnetization of the sample in the external magnetic field often sets in the way of two concomitant mechanisms of restructurization of the magnetic moments of the solid particles: one is that of magnetization relaxation related to the Brownian rotation of the particles in the carried liquid, whereas the other one consists in thermal fluctuations of the magnetic moment within the particle itself.

2. Characteristic of magnetic liquids

2.1. Static magnetic properties

The dispersive phase of magnetic liquids consists of ferri- or ferromagnetic particles that undergo strong magnetization already in rather weak fields. In condensed ferromag-netics, there arise elementary regions of spontaneous magnetization — domains in that the spontaneous magnetization attains saturation.

The external magnetic field reorients the elementary magnetic moments in the sam-ple, so that it exhibits magnetization.

When the field is switched off, the magnetization M of the system of particles tends to zero due to the thermal motion of the magnetization vectors $\mathbf{m}$ of the individual particles.

The time-dependent decrease of M obeys the law of exponential decay [1],

$$M = M_\infty \exp\left(-\frac{\tau}{\tau_N}\right), \qquad (1)$$

where τ_N is *the relaxation time of magnetization* due to the mechanism proposed by Néel. In accordance with the model of discrete orientation of the vector $\mathbf{m}$, the Néel relaxation time τ_N is given by the following equation [1, 2]:

$$\tau_N = \tau_0 \exp\left(\frac{K_1 V}{kT}\right), \qquad (2)$$

where τ_0 — time of Larmor precession of the vector $\mathbf{m}$ around the anisotropy axis, K_1 — anisotropy constant of the single crystallographic axis, V — mean volume of the magnetic particle, kT — thermal energy of the magnetic particle.

In this case, the magnetic moment can change its direction within an immobile magnetic grain overcoming the energy barrier $K_1 V$.

For magnetite Fe_3O_4, a component of the magnetic liquid EMG-605 studied by us, the parameter $K_1 = 11\,\text{kJ/m}^3$. For the mean radius of a single magnetic particle $r = 10\,\text{nm}$, which corresponds to a mean volume of $4.2 \cdot 10^{-24}\,\text{m}^3$, we get for the potential energy $4.6 \cdot 10^{-20}\,\text{J}$.

The time τ_0 results from the Larmor precession of the vector $\mathbf{m}$ around the anisotropy axis; various authors [2, 3] have assumed $\tau_0 \simeq 10^{-9}\,\text{s}$. With this in mind, and at $T = 293\,\text{K}$, the Néel magnetization relaxation time can be assessed at $\tau_N = 98\,\mu\text{s}$.

The intensity of Brownian diffusion of the vector $\mathbf{m}$ is given by the energy kT.

The static state of the particle depends on the ratio of two parameters, $\sigma_N = K_1 V/kT$ and $\xi = \mu_0 m H/kT$, which characterize the mutual relation between the energies of magnetic anisotropy and interaction with the external magnetic field and the energy of thermal motion. The numerator $\mu_0 m H$ means the magnetic energy of the magnetic particle with magnetic dipole moment $\mathbf{m}$ in the external magnetic field strength H; μ_0 is the permeability of the free space and has the value of $4\pi \cdot 10^{-7}\,\text{H/m}$.

If $K_1 V \ll kT$ and $K_1 V \ll \mu_0 m H$, the orientation of the vectors $\mathbf{m}$ of the individual particles varies randomly about the field vector under the action of thermal fluctuations which damp the resultant field.

The relaxation time τ_N is the decay time of the Larmor precession τ_0 of the magnetic moment. In this case, the crystallographic anisotropy can be neglected, the external symptoms of a ferromagnetic material vanish, and the hysteresis loop goes over into a simple magnetization curve ($B_r = 0$ and $H_c = 0$) which obeys the Langevine law,

$$M = M_s \left(\coth \frac{\mu_0 m H}{kT} - \frac{kT}{\mu_0 m H} \right). \tag{3}$$

In this case B_r and H_c mean remanence and coercivity of the material, respectively, whereas M_s is the magnetization at $H \to \infty$.

As mentioned above, the colloidal particles of a ferro- or ferrimagnetic material possess a magnetic moment of constant magnitude dependent on the magnetization M_s and the volume V of the particle. The external magnetic field aligns the magnetic moments, leading to magnetization on a macroscopic scale in the sample.

The orientation of the magnetic moments of the colloidal particles proceedes according to two mechanisms:

(i) Inside the monoaxial particle of the solid, thermal reorientation of the magnetic moment takes place between two opposite directions of the easy magnetization axis of the crystal.

(ii) The particles undergo rotation with respect to the carrier as a result of thermal motion.

In the absence of a magnetic dipole interaction between monodisperse colloidal particles, the magnetic state of the medium is described by the classical law derived by Langevin for the magnetization of molecules of a paramagnetic gas,

$$\frac{M}{M_\infty} = \frac{M}{M_s \phi_M} = \coth \xi - \frac{1}{\xi} \equiv L(\xi), \tag{4}$$

with ϕ_M the volume concentration of the magnetic material and $\xi = \mu_0 mH/kT$ the argument of the Langevin function $L(\xi)$.

For spherical particles of diameter d, the argument of the Langevin function takes the form: $\xi = \pi\mu_0 M_s H d^3 /6kT$.

Figure 1 shows the Langevin function $L(\xi)$ *versus* the external magnetic field strength H for spherical magnetic particles with radii of 2.5 nm, 5 nm and 10 nm. We assumed the following values for the magnetization saturation $M_s = 478\,\text{kAm}^{-1}$ and the volume concentration $\phi_M = 3.5\%$ which correspond to the magnetic liquid EMG-605 used in our experimental work.
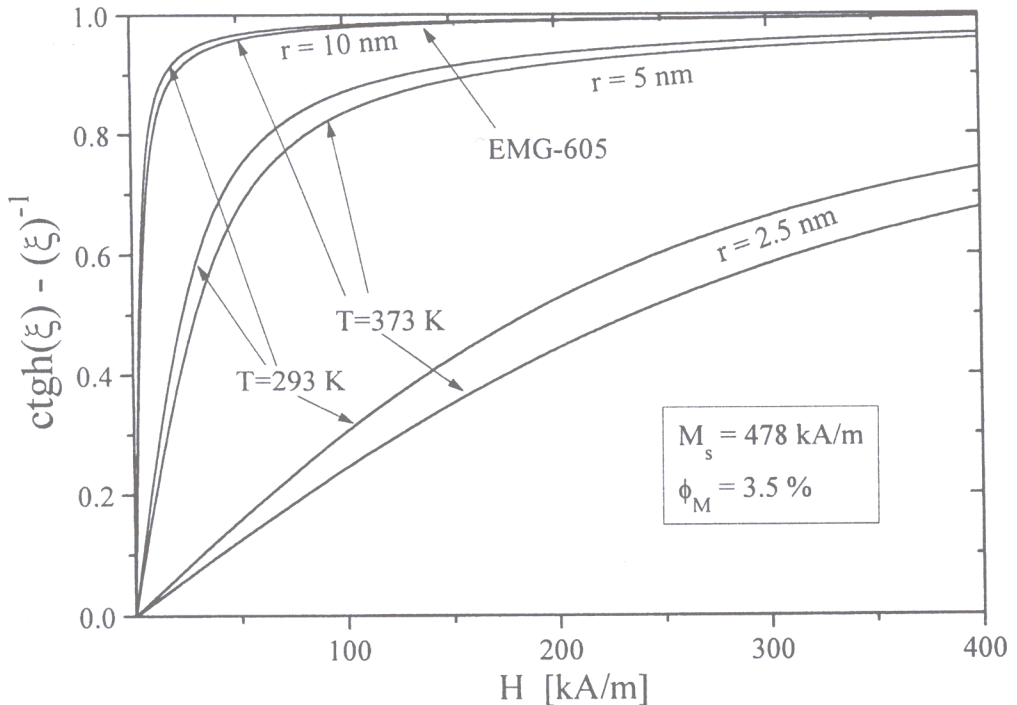

Fig. 1. Langevin function of magnetite magnetic liquids with magnetic grains of different radii *versus* the magnetic field strength at $+20°\text{C}$.

Figure 1 shows that the liquid achieves magnetic saturation at about $50\,\text{kAm}^{-1}$, whereas the temperature affects the state of magnetization but weakly.

Now, real magnetic liquids have a well defined degree of polydispersion of the solid phase, causing some slight discrepancy between the experimental points and the magnetization curve plotted according to the Langevin's law [4]. This discrepancy is due mainly to the effect of larger particles.

Another property typical of systems of noninteracting single-domain particles is displayed by the simple $M(H/T)$ curve, i.e. by the lack of hysteresis of the magnetization.

The formation of aggregates in the magnetic liquid and the increase in the diameter of the monodisperse particles should affect the magnetization curve qualitatively.

With increasing mean diameter, an increase in the formation of aggregates is observed, the smaller particles tending to penetrate between the greater ones and leading to a packing of the aggregates that is more dense than that of a monodisperse system. The arisen aggregates cause an increase in the magnetization of the liquid of monodisperse particles, as well as an effect related to the increase of the effective size of the particles in the disperse phase.

2.2. The kinetics of magnetization

The process of magnetization of a magnetic liquid is ruled by two mechanisms:

(i) the mechanism of magnetization relaxation related to Brownian rotations of the particles in the carrier liquid,

(ii) the mechanism involving thermal fluctuations of the magnetic moments within the particles themselves.

Either of the processes is characterized by a specific relaxation time.

The Brownian rotational diffusion time of the colloidal particles is given by the expression [1, 5],

$$\tau_B = \frac{3V\eta_0}{kT},\tag{5}$$

where η_0 is the dynamical viscosity of the carrier liquid, and V the hydrodynamic volume of the grain. Quite generally, the two mechanisms can run simultaneously when the external field is switched on, the magnetization vector of a given magnetic particle rotating at a greater velocity than the particle itself. In this case, the effective time constant of the magnetization process is smaller than both the components and can be determined from the following expression [1, 3, 5]:

$$\tau_{\text{eff}} = \frac{\tau_N \cdot \tau_B}{\tau_N + \tau_B}.\tag{6}$$

If $\tau_N \ll \tau_B$, the magnetization relaxation process is related to the Néel mechanism. If the opposite is the case ($\tau_N \gg \tau_B$), the equilibrium orientation of the magnetic moments sets in chiefly by the way of Brownian rotations of the particles.

The transition from one of the relaxation mechanisms to the other one can be found by comparing the expressions (2) and (5).

If the magnetic liquid with an aqueous carrier freezes (the magnetic particles are blocked), Brownian rotation will not occur ($\tau_B \nearrow \infty$). In this case the effective relaxation time of the magnetic susceptibility $\tau_{\text{eff}} = \tau_N$. These small single-domain magnetic particles are sometimes referred to as superparamagnetic. In this region of the radii, one of the mechanisms can predominate.

Figure 2 shows the effective relaxation time of the magnetic susceptibility *versus* the radius of a spherical particle of magnetite together with the two components originating in the respective mechanisms. The graph was plotted for a water-based magnetic liquid at 293 K. Obviously, for particles with a radius of about 8.7 nm the two mechanisms participate equally.

Moreover, it is assumed that in the liquid studied (EMG-605, $r = 10$ nm), the Brownian magnetization mechanism strongly predominates.
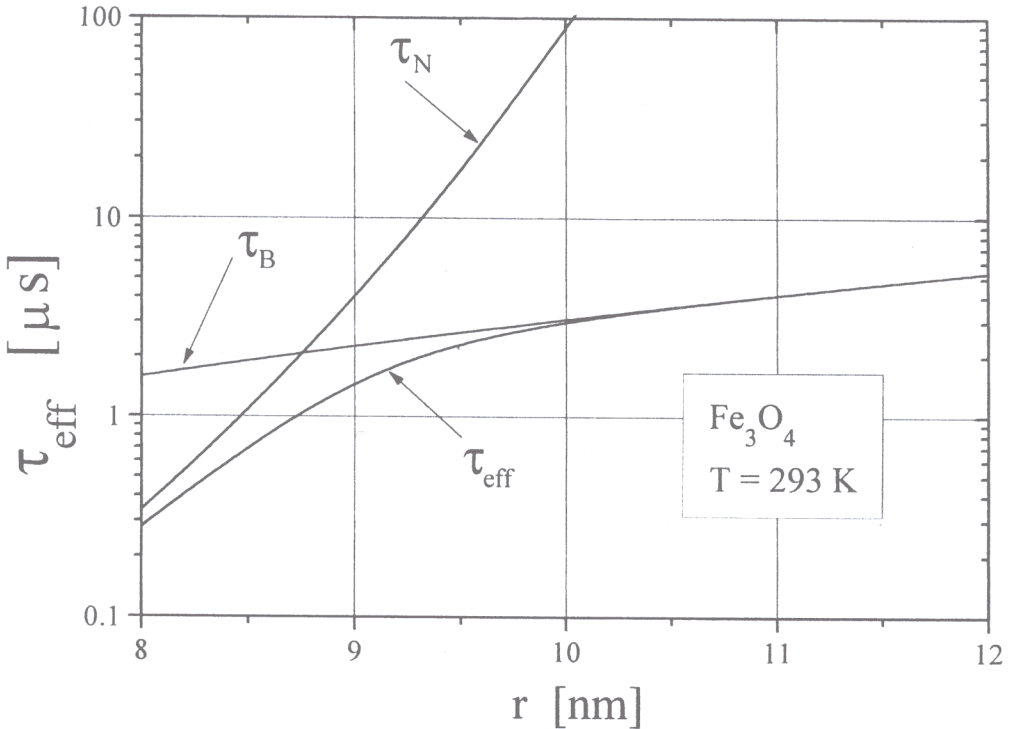
Fig. 2. Effective relaxation time of the magnetic susceptibility and its components *versus* the radius of a spherical magnetite grain at +20°C.

In this case, the effective relaxation time of the magnetic susceptibility $\tau_{\text{eff}} \simeq \tau_B$, since τ_B is about 30 times shorter than τ_N. However, it would suffice to use a magnetic liquid with smaller magnetic grains (say, with $r = 5$ nm) and the system would magnetize according to the Néel's mechanism.

In reality, only a small portion of the grains in EMG-605 magnetizes according to the Néel mechanism because of its polydisperseness.

One of the methods of experimental determination of the characteristic relaxation times is to measure the complex magnetic susceptibility of the liquid with an AC magnetic field as a function of frequency. In such a field the magnetization undergoes a delay in phase with regard to the field strength, thus causing a change in the resultant magnetic moment that proceeds at a finite rate.

In sufficiently weak magnetic fields varying in time harmonically, the magnetic susceptibility can be written in the complex form [3, 6],

$$\tilde{\chi}(\omega) = \chi'(\omega) - i\chi''(\omega) = \chi_\infty + \frac{\chi_0 - \chi_\infty}{1 + i\omega\tau_0}, \qquad (7)$$

where χ' — describes the reversible magnetization processes, χ'' — characterizes the processes of dissipation of the magnetic field energy, and $\omega = 2\pi f$ the angular frequency.

The time constant $\tau_0 = (2\pi f_m)^{-1}$ determines the frequency at which dissipation of the magnetic field energy becomes maximum, whereas the quantities χ_∞ and χ_0 denote respectively the susceptibility at infinitely high frequency of the magnetic field and in a constant magnetic field.

The latter can be written as:

$$\chi_0 = \frac{\mu_0 n m^2}{3kT},\tag{8}$$

where n is the density of the magnetic particles with a magnetic moment m. The Debye's rule describes the dependencies of the real and imaginary parts of the complex electric permittivity of a dipolar liquids on the angular frequency $\omega = 2\pi f$ of the externally applied electric field and the relaxation time τ_0.

The application of this rule for the description of magnetic liquids is based on the hypothesis of the exponential increase of magnetization when the magnetic field is switched on. As in the Debye's theory, the real part of the magnetic permittivity decreases monotonically:

$$\chi'(\omega) = \chi_\infty + \frac{\chi_0 - \chi_\infty}{1 + \omega^2 \tau_0^2},\tag{9}$$

wheras the imaginary part has a maximum at $\omega\tau_0 = 1$ and amounts to

$$\chi''(\omega) = (\chi_o - \chi_\infty)\frac{\omega\tau_0}{1 + \omega^2 \tau_0^2}.\tag{10}$$

Hence, the relaxation time can be found once we have determined experimentally the frequency at which the imaginary part of the permittivity appears. However, the dispersion equation of Debye holds only as long as we deal with a simple model with a single relaxation time and if intermolecular interactions can be neglected.

In real polydisperse magnetic liquids dispersion of the magnetic permittivity described more adequately by the following formula [3, 7] containing the distribution function of the permittivity relaxation times $f(\tau)$:

$$\tilde{\chi}(\omega) = \chi'(\omega) - i\chi''(\omega) = \chi_\infty + (\chi_0 - \chi_\infty)\int\limits_0^\infty \frac{f(\tau)d\tau}{1 + i\omega\tau}.\tag{11}$$

In most cases one can proceed by fitting the experimental results to the following function [7]:

$$\tilde{\chi}(\omega) = \chi_\infty + \frac{(\chi_0 - \chi_\infty)}{1 + (i\omega\tau_0)^{1-\alpha}},\tag{12}$$

where the parameter α takes values from the interval $0 \leq \alpha \leq 1$. For $\alpha = 0$, equation (12) goes over into the Debye's equation.

In the complex χ', χ'' plane (Cole-Cole diagram), the above dependence is represented by an arc of a semicircle with centre at the point $[0.5(\chi_0+\chi_\infty), -0.5(\chi_0-\chi_\infty)\,\mathrm{tg}(\pi\alpha/2)]$ and with the radius $R = 0.5(\chi_0 - \chi_\infty)\sec(\pi\alpha/2)$. Consequently, the centre of the semicircle lies below the axis of real values of the magnetic permittivity.

3. Propagation of an ultrasonic wave in a magnetic liquid

The theory proposed by TAKETOMI [8], who considered the anisotropy of the absorption coefficient of the ultrasonic wave propagating in a magnetic liquid, proved to be much more effective than the theories of other authors [9, 10].

Magneto-optical experiments have shown that in a magnetic liquid affected by an external constant magnetic field clusters of approximately spherical shape arise.

Their size depends on the radius of the individual magnetic particles, the strength of the magnetic field and the temperature. With growing field strength, the spherical clusters tend to form chains lying along the magnetic field lines and enhancing in this way the stiffness of the liquid.

The energy of an ultrasonic wave propagating in such a medium is converted into the energy exciting the translational and, consequently, the rotational degrees of freedom of the clusters.

Thus the amplitude absorption coefficient of the ultrasonic wave propagating in a magnetic liquid placed in an external magnetic field consist of a part related to the rotational motion of the clusters, α_r, and a translational part α_t [8]:

$$\alpha_r(\phi) = \frac{\omega^2}{2\varrho_0 c^3}\left(\frac{4\eta_s}{3} + \eta_v + 2\alpha_5\cos^2\phi + \alpha_1\cos^4\phi\right), \tag{13}$$

$$\alpha_t(\phi) = \frac{1}{ck^2}\cdot\frac{3\pi\eta_s r\omega^3 VN(6\pi r\eta_s + V\omega\varrho_0)}{\left(\sin\phi - \dfrac{V\omega^2\varrho_m}{k}\right)^2 + \left(\dfrac{6\pi r\omega\eta_s}{k}\right)^2}, \tag{14}$$

where c is the velocity of the ultrasonic wave of angular frequency ω, ϱ_0 and ϱ_m are the densities of the carrier liquid and magnetic particles, respectively, η_s and η_v are the dynamic and volume viscosities, r and V are the radius and volume of the cluster, N is the number of clusters per unit volume, k is the elasticity constant of the magnetic liquid, ϕ is the angle between the magnetic field strength vector and the propagation vector of the ultrasonic wave, and α_1 and α_5 are the Leslie coefficients appearing in the theory of liquid crystals [14].

On adjusting the function $\alpha_r(\phi) + \alpha_t(\phi)$ to the experimentally determined values of the anisotropy of the absorption coefficient of the ultrasonic wave in the magnetic liquid, we obtain information concerning the following physical quantities: $(4\eta_s/3 + \eta_v)$, α_1, α_5, r, k and N. On the assumptions made by Taketomi, the spherical clusters should be packed homogeneously and should be of equal size which not always takes place exactly. This e.g. may be due to the polydispersion of the magnetic particles resulting in the formation of grains of different size. Thus there is a lack of ideal packing. Due to the polydispersion of the magnetic liquid, grains with a greater diameter are more apt to coagulate than the smaller ones.

However, this tendency is opposed by thermal vibrations the energy of which, kT, is a function of the absolute temperature.

Magnetostatic considerations [11] lead to the conclusion that the energy E_{dd} required to separate two coagulated magnetic grains depends on their size and magnetic properties

according to the formula:

$$E_{dd} = \frac{\mu_0 M_s^2 V}{12},$$ (15)

where M_s is the spontaneous magnetization of the magnetic particle and V its volume.

The coagulation coefficient λ of the magnetic grains, defined as the quotient of the interdipole interaction energy E_{dd} and the thermal energy kT, affects the stability of the magnetic liquid essentially.

If $\lambda > 1$, the magnetic liquid can coagulate spontaneously according to the external magnetic field applied.

Figure 3 shows $\lambda(r)$ for magnetite *versus* three temperatures $T = 273$, 293 and 373 K, thus in a temperature range accessible to the magnetite liquid with the aqueous carrier. The temperature was found to have some influence on λ which, however, is very depends strongly on the radii of the magnetic particles.
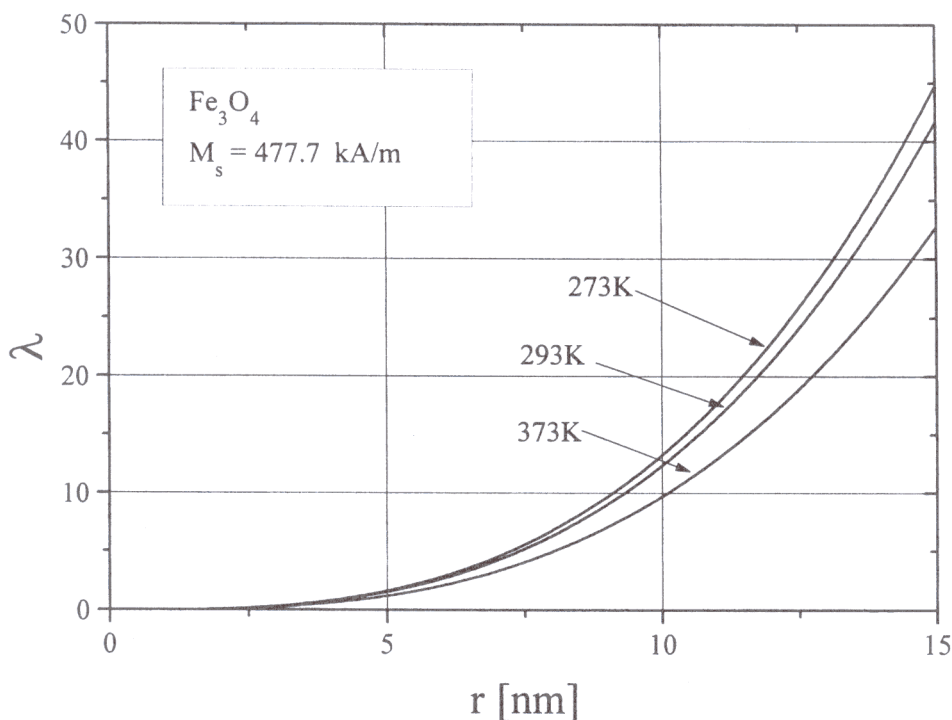

Fig. 3. Coupling coefficient of the magnetite grains $\lambda(r)$ *versus* their radius for $T = 273$ K, 293 K and 373 K.

For $\lambda < 1$ ($r < 4.5$ nm), the energy of thermal vibrations exceeds that of two dipoles in conjunction; such a monodisperse liquid should be stable. In the case of the polydisperse magnetic liquid used in our experiments, in that the mean radius amounted to 10 nm, depending on the temperature, an effective value of $\lambda = 9 \div 14$ was obtained. This points to the possibility of spontaneous coagulation.

4. Experimental

4.1. Measuring setup for the determination of the anisotropy of the absorption coefficient of ultrasonic waves

The measuring setup for the determination of the anisotropy of the absorption coefficient of the ultrasonic wave, shown in Fig. 4, consisted of subcircuits made by "MATEC". The apparatus operated on the pulse principle involved additionally a block type "MODEL 2470B" with time — delay circuits operating on the pulses of consecutive echos and two channels with analog memories in that the magnitudes of these echos were stored.
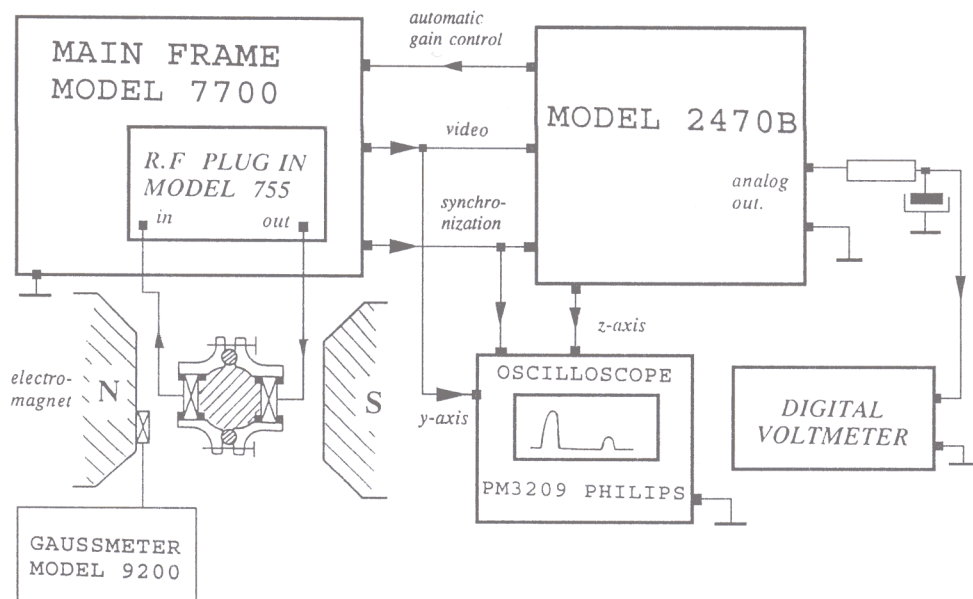

Fig. 4. Measuring setup for the determination of the anisotropy of the ultrasonic absorption coefficient.

Hence both the constant voltage electric signals, proportional to the amplitudes of the memorized echos, were fed to a logarithmic amplifier; the output voltage of the latter was thus proportional to the amplitude absorption coefficient of the ultrasonic wave in the medium under investigation. The measurement accuracy was $\pm 0.02\,\mathrm{cm}^{-1}$. The measurement of the magnetic field induction in the slit of the electromagnet between its poles was performed with an accuracy of 0.5% using a teslometer.

The temperature of the medium was stabilized to within $\pm 0.01\,\mathrm{K}$.

4.2. Measuring apparatus for the determination of the magnetic succeptibility

To determine the magnetic properties of the magnetic liquid, a Maxwell–Wien bridge (see Fig. 5) was used. The AC magnetic field applied to the cell with the magnetic fluid is perpendicular to the direction of the DC magnetic field.
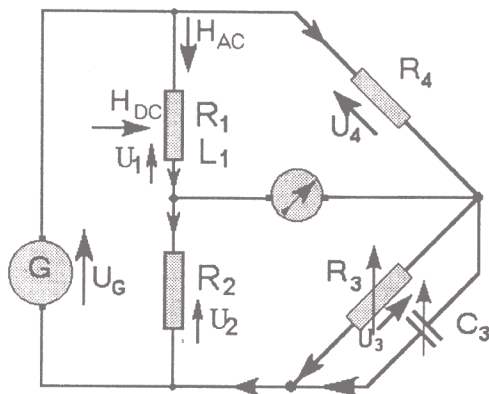
Fig. 5. Maxwell-Wien bridge for the determination of the susceptibility of EMG-605.

The bridge was fed from a generator providing a sine voltage signal of controlled amplitude and frequency. One of the branches of the bridge contained the glass vessel having the shape of a ring (Rowland ring) and holding about $3\,\mathrm{cm^3}$ of the magnetic liquid. The branch opposite the Rowland ring consisted of a capacitance decade and resistor decade and served to equilibrate the bridge.

This was checked with a milivoltmeter (at higher frequencies, a diode probe was used additionally). The two remaining branches were constructed with inductionless standard resistors $(61.9\,\Omega)$. All the elements of the bridge were constructed with screened cables so that the range of measurements could be easily extended to a frequency of $100\,\mathrm{kHz}$, whereas a standard use of the bridge covers $5\,\mathrm{kHz}$ only.

Upwards of $100\,\mathrm{kHz}$, a skin effect and parasitic currents of volume type began to affect the measurements, in the first case causing an error in the imaginary part of the magnetic susceptibility and in the second one an error in its real part.

With the bridge equilibrium, the following identity is fulfilled:

$$R_2 R_4 = (R_1 + j\omega L_1)\left(\frac{R_3}{1 + j\omega C_3 R_3}\right),\tag{16}$$

whence it results that the resistance and inductance provided by the coil on the ring, the magnetic circuit being closed by the magnetic liquid, amount to

$$R_1 = \frac{R_2 R_4}{R_3}, \qquad L_1 = R_2 R_4 C_3.\tag{17}$$

If L_{10} is the inductance of the empty coil, we get an expression for the real part of the magnetic susceptibility:

$$\chi' = \frac{L_1 - L_{10}}{L_{10}},\tag{18}$$

with an accuracy of the order of 0.2% [12].

5. Experimental results

The measurements have been performed for a magnetic liquid with the symbol EMG-605 made by Ferrofluidics Corporation. It consists of magnetite Fe_3O_4 grains with a mean radius of 10 nm suspended in water serving as the carrier liquid.

The values of the magnetization, initial magnetic susceptibility, dynamic viscosity and volume concentration of the magnetic liquid were 20 mT, 0.55, 0.005 Nsm^{-2} and 3.5%, respectively.

The values of density, spontaneous magnetization, crystal lattice constant, uniaxial crystallografic anisotropy constant and ferromagnetic Curie point of the magnetite Fe_3O_4 were 5240 kgm^{-3}, 477.7 kAm^{-1}, 0.84 nm, 11 kJm^{-3} and 585° C, respectively.

The anisotropy of the ultrasonic wave absorption coefficient in the magnetic liquid EMG-605 was measured at 20° C, at a constant magnetic field strength (the parameter), and the frequency of 4.38 MHz.

As an example, the dependence of the ultrasonic absorption coefficient in EMG-605 versus the angle ϕ at 20° C for several constant values of the magnetic field strength H is shown in Fig. 6.

The magnetic susceptibility of EMG-605 was measured versus the frequency f of the variable magnetic field component H_{AC} at a constant magnetizing field H_{DC} (the parameter).
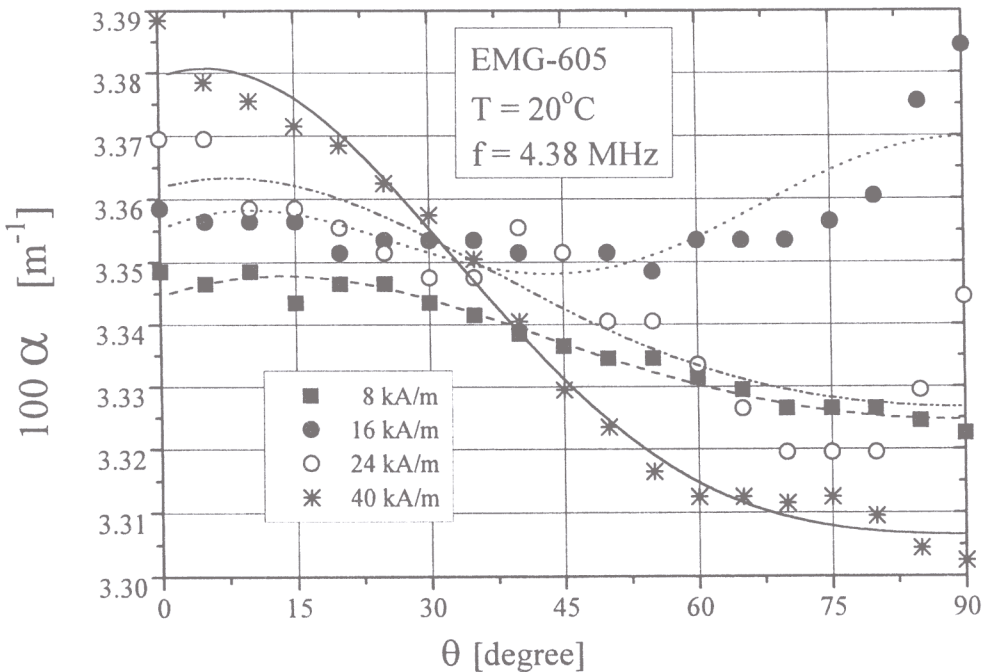

Fig. 6. Anisotropy of the ultrasonic absorption coefficient together and the curves obtained by fitting the experimental data to the Taketomi function at constant magnetic field strengths $H = 8, 16, 24$ and 40 kA/m.
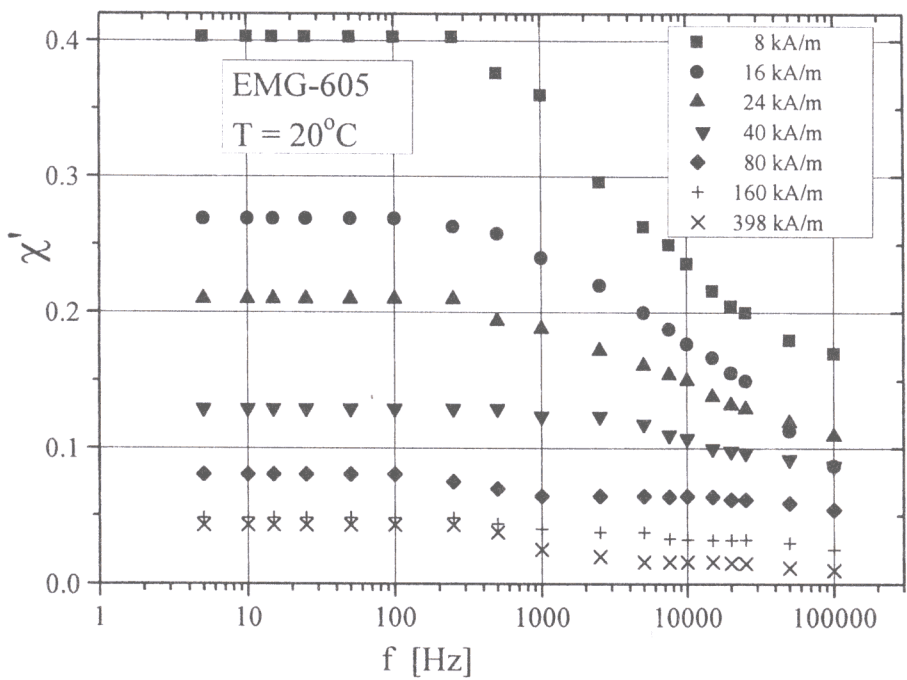
Fig. 7. Real component of the magnetic susceptibility χ' of EMG-605 *versus* frequency f of the variable magnetic field component H_{AC} at constant values of H_{DC}.
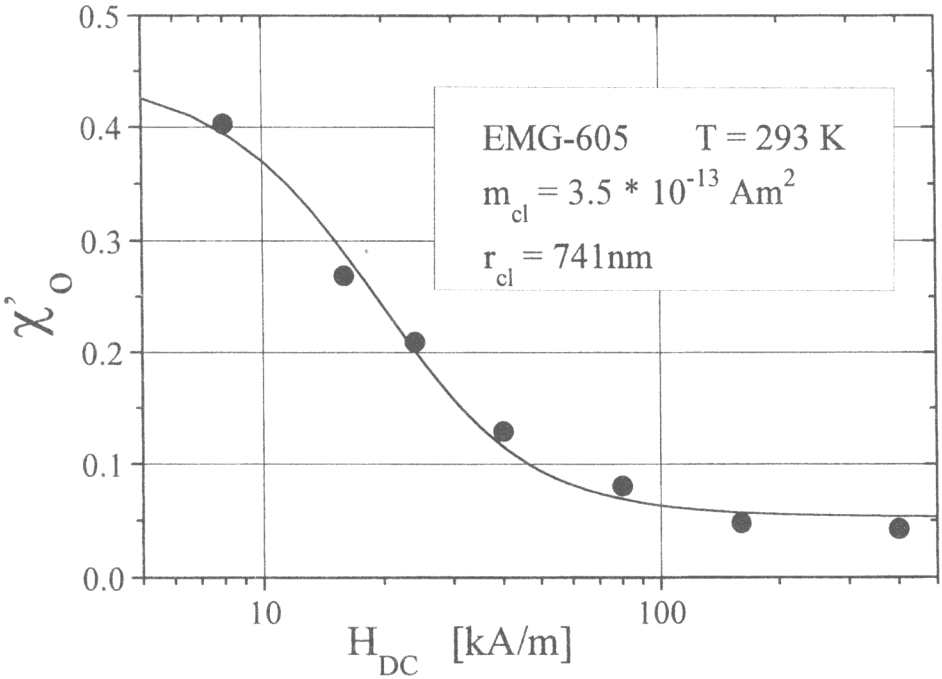

Fig. 8. Real component of the initial magnetic susceptibility χ'_0 *versus* H_{DC} and the curve resulting from the fitting to function [13] for the magnetic liquid EMG-605.

The frequency ranged from 5 to 100 kHz, whereas H_{DC} was 8, 16, 24, 40, 79.6, 159.2 and 398 kAm^{-1}. The measurements were carried out at $T = 20°$ C. Figure 7 shows the real component of the susceptibility χ' of EMG-605 *versus* the frequency f of the variable field component H_{AC} for H_{DC} values maintained constant. Additionally, Fig. 8 shows the real component of the initial susceptibility χ'_0 of EMG-605 *versus* H_{DC}.

6. Analysis of the results, and conclusions

The curves plotted in Fig. 6 were obtained by adjusting Taketomi's function to the experimental data of the absorption coefficient of the ultrasonic wave in the magnetic liquid. This adjustment enabled the determination of the values of the quantities describing the structure of the magnetic liquid as shown in Table 1.

Table 1. Results obtained by adjusting the Taketomi function to the experimental data of the absorption coefficient of the ultrasonic wave in the magnetic liquid EMG-605 at $T = 20°$C.

H	$4\eta_s/3 + \eta_v$	α_5	α_1	r	k	$N \times 10^{-16}$
kA/m	mPa·s	mPa·s	mPa·s	μm	N·m^{-1}	m^{-3}
8	13.90	−0.121	0.099	3.67	3.90	80.6
16	14.41	−0.63	0.654	3.71	4.81	78.2
24	18.02	−0.165	0.165	3.37	4.75	71.1
40	18.57	−0.417	0.430	3.37	7.00	69.7

When analyzing the results of our ultrasonic studies, one notes that an increase in the magnetic field strength causes:

(i) an increase in the viscosity coefficient $4\eta_s/3 + \eta_v$,

(ii) an increase in the magnitude of the elasticity constant of the magnetic liquid k, and

(iii) a decrease in the number of clusters N per unit volume of the liquid.

According to the single relaxation time model, the measuring points of magnetic susceptibility $\chi'(\omega)$ shown in Fig. 7 should coincide with the function of the complex magnetic susceptibility resulting from the Langevin's law [13],

$$\chi(\omega, H_0) = \frac{\chi_0[1 + f(H_0)]}{1 + j\omega\tau_{\text{eff}}}, \tag{19}$$

where the numerator amounts to

$$[1 + f(H_0)] = 3\left[1 + \xi^{-2} - \coth^2\xi\right]. \tag{20}$$

Thus, the function expressing the real part of the magnetic susceptibility, $\chi'(\omega, H_0)$, should be of the form,

$$\chi'(\omega, H_0) = \frac{\chi_0[1 + f(H_0)]}{1 + \omega^2\tau_{\text{eff}}^2}, \tag{21}$$

where τ_{eff} is the effective relaxation time of the magnetic susceptibility.

In reality, the attempts to adjust the functions with a single relaxation time to the above experimental results failed. Whereas the application of an adjusting function with two relaxation times [6]

$$\chi(\omega) = \chi_{\infty 2} + \frac{\chi_0 - \chi_{\infty 1}}{1 + i\omega\tau_1} + \frac{\chi_{\infty 1} - \chi_{\infty 2}}{1 + i\omega\tau_2},$$ (22)

permitted the achievement of good results as shown by the relaxation data given in Table 2.

Table 2. Results obtained by adjusting the magnetic susceptibility function with two relaxation times to the experimental data for the magnetic susceptibility of EMG-605 at $T = 20°$ C.

H	$\chi_0 - \chi_{\infty 1}$	τ_1	$\chi_{\infty 1} - \chi_{\infty 2}$	τ_2	$\chi_{\infty 2}$	χ_0
kA/m	–	µs	–	µs	–	–
8	0.1444	107	0.089	9.3	0.1692	0.4026
16	0.083	69.2	0.1076	4.57	0.076	0,2666
24	0.0393	210	0.0532	12.75	0.117	0.2094
40	0.03	24	0.014	3.47	0.084	0.128

In the case of the weakest magnetic field used in the measurements, $H = 8\,\mathrm{kAm^{-1}}$, the relaxation times $\tau_1 = 107\,\mu s$ and $\tau_2 = 9.3\,\mu s$ coincide quite satisfactorily with the components of the effective relaxation time of the magnetic susceptibility shown in Fig. 2 in accordance with the effects of Brown and Néel.

Finally, Fig. 8 shows the measuring points obtained for the real component of the initial magnetic susceptibility χ_0' versus H_{DC} together with the curve of fitting to the function (20). This adjustment led to a limiting value of $\chi_0' = 0.43$ for the real component of the initial magnetic susceptibility and to the mean radius of the magnetic clusters $r_{cl} = 741\,\mathrm{nm}$.

Acknowledgements

References

[1] R. KÖTITZ, P.C. FANNIN, L. TRAHMS, *Time domain study of Brownian and Néel relaxation in ferrofluids*, J. Magn. Magn. Mater., **149**, 42–46 (1995).

[2] P.C. FANNIN, S.W. CHARLES, *On the calculation of the Néel relaxation time in uniaxial single-domain ferromagnetic particles*, J. Phys. D: Appl. Phys., **27**, 185–188 (1994).

[3] P.C. FANNIN, YU.P. KALMYKOV, S.W. CHARLES, *On the use of frequency-domain measurements to investigate time-domain magnetization decay in a ferrofluid*, J. Phys. D: Appl. Phys., **27**, 194–197 (1994).

[4] W. FERTMAN, *Magnetic liquids* [in Russian], High School, Minsk 1988.

[5] P.C. FANNIN, S.W. CHARLES, T. RELIHAN, *Broad-band measurement of the complex susceptibility of magnetic fluids*, Meas. Sci. Technol., **4**, 1160–1162 (1993).

[6] P.C. FANNIN, S.W. CHARLES, T. RELIHAN, *On the use of complex susceptibility data to complement magnetic viscosity measurements*, J. Phys. D: Appl.Phys., **27**, 189–193 (1994).

[7] E. BLOOMS, A. CERBERS, M.M. MAIOROV, *Magnetic fluids*, Walter de Gruyter, Berlin, New York 1997.

[8] S. TAKETOMI, *The anisotropy of the sound attenuation in magnetic fluid under an external magnetic field*, J. Phys. Soc. Jpn., **55**, 838–844 (1986).

[9] K. GOTOH, D. CHUNG, *Ultrasonic attenuations in magnetic fluids*, J. Phys. Soc. Jpn., **53**, 8, 2521–2528 (1984).

[10] K. HENJES, *Sound propagation in magnetic fluids*, Phys. Rev. E, **50**, 2, 1184–1188 (1994).

[11] R.E. ROSENSWEIG, *Ferrohydrodynamics*, Dover Publications, INC., Mineola, New York 1997.

[12] A. JELLONEK, J. KURYŁOWICZ, M. ŁAPIŃSKI, Z. SICIŃSKI, *Electrical measurements*, PWN, Warszawa 1971, pp. 244–245.

[13] P.C. FANNIN, B.K.P. SCAIFE, S.W. CHARLES, *The field dependence of the complex frequency-dependent susceptibility of magnetic fluids*, J. Phys. D: Appl. Phys., **21**, 533–534 (1988).

[14] P.G. GENNES, *The physics of liquid crystals*, Oxford University Press, London 1975.